ma
the
ma
tisch

cen
trum

AFDELING NUMERIEKE WISKUNDE
(DEPARTMENT OF NUMERICAL MATHEMATICS)

NW 122/82 JANUARI

P.W. HEMKER

MIXED DEFECT CORRECTION ITERATION FOR THE ACCURATE SOLUTION OF THE CONVECTION DIFFUSION EQUATION

Preprint

amsterdam 1982

stichting
mathematisch
centrum

MC

AFDELING NUMERIEKE WISKUNDE
(DEPARTMENT OF NUMERICAL MATHEMATICS)

NW 122/82 JANUARI

P.W. HEMKER

MIXED DEFECT CORRECTION ITERATION FOR THE ACCURATE SOLUTION OF THE CONVECTION DIFFUSION EQUATION

Preprint

kruislaan 413 1098 SJ amsterdam

Printed at the Mathematical Centre, 413 Kruislaan, Amsterdam.

The Mathematical Centre, founded the 11-th of February 1946, is a non-profit institution aiming at the promotion of pure mathematics and its applications. It is sponsored by the Netherlands Government through the Netherlands Organization for the Advancement of Pure Research (Z.W.O.).

1980 Mathematical subject classification: 65N05, 65N10

Mixed defect correction iteration for the accurate solution of the convection diffusion equation*)

by

P.W. Hemker

ABSTRACT

In this report, a continuation of research described in report NW 117/81, a further analysis is given of the Mixed Defect Correction iteration method. First the iteration method is described for application to the convection-diffusion equation in two dimensions. Then the convergence of the iteration process is studied. Further, an analysis of the down-stream boundary layer behaviour is given and numerical results are shown, when the method is applied to some model problems.

KEYWORDS & PHRASES: *Defect correction, convection-diffusion equation Singular perturbation problem*

---

*) This report will be submitted for publication elsewhere.

1. INTRODUCTION

In this paper we study properties of an iteration scheme for the numerical solution of the convection-diffusion equation

$$(1.1) \qquad L_\varepsilon u \equiv -\varepsilon \Delta u + \vec{a}.\nabla u = f,$$

in two dimensions, in particular in the case of a small diffusion coefficient ε. For small ε the equation is dominated by the convection term and boundary- or interior layers may appear along or downstream the convection direction $\vec{a}$. If the meshwidth of a discretization h is small compared with the thickness of these layers, standard methods for the numerical solution of (1.1) may fail to be efficient. Accurate methods such as finite element discretizations with piecewise polynomials become unstable for small ε/h, whereas stable methods, such as obtained by upwinding or application of artificial diffusion, are only 1st order accurate.

A proper mesh-refinement in the boundary layers may solve many of these problems in practice, but it requires a priori knowledge about the location and the shape of the boundary layer. For the automatic solution of (1.1) we seek a method (i) which does not make use of a-priori knowledge about the solution, (ii) of which the discretization is independent of a convection direction $\vec{a}$, (iii) which is accurate $O(h^2)$ in the smooth parts of the solution and (iv) which locates the boundary and interior layers properly. Further we want that the width of the numerical boundary layer is at most $O(h)$ for small values of ε/h. Such a method is suited for application in an algorithm which resolves the boundary layers by adaptive mesh-refinement.

We propose an iteration scheme that satisfies the above requirements and that can readily be incorporated in an iteration scheme for the solution of the discretized system. The method is based on an idea by BRANDT (1980) to increase the order of accuracy of a discrete solution in a multilevel algorithm by computing the residual - for transfer to a coarser grid - relative to a more accurately discretized operator than the operator that is used for the relaxation. This idea is very much related to the defect correction principle (see e.g. STETTER (1978), HACKBUSCH (1979), HEMKER (1981, 1982)).

Although we apply our method also to problems (1.1) with variable coefficients $\vec{a} = \vec{a}(x,y)$ in section 5, we restrict the analysis to the problem with constant coefficients. In order to show some details of a computation we also resort to the

simple one-dimensional problem

$$\varepsilon y'' + 2y' = f. \tag{1.2}$$

As was indicated by BRANDT (1980), the one-dimensional problem has properties that can not be generalized to more dimensions. However, some basic techniques that are used in the 2-D case are more easily shown with the 1-D example.

In this paper the same method is used for the solution of (1.1) as was used in HEMKER (1982). In the present paper we extend previous results with a treatment of the convergence properties of the iteration and of the behaviour of the solution in the neighbourhood of the boundary. Also, some additional numerical results are presented.

2. THE ELEMENTARY DISCRETIZATIONS

For the discretization of the equation (1.1) we essentially use only a simple finite element or finite difference discretization. The analysis is made for the discretization on a regular square grid. In this case the difference stars are given by

$$L_{h,\varepsilon} = \frac{-\varepsilon}{h^2}\begin{bmatrix} & 1 & \\ 1 & -4 & 1 \\ & 1 & \end{bmatrix} + \frac{a_1}{(4+2p)h}\begin{bmatrix} & -p & +p \\ -2 & 0 & 2 \\ -p & p & \end{bmatrix} + \frac{a_2}{(4+2p)h}\begin{bmatrix} & +2 & p \\ p & 0 & -p \\ -p & -2 & \end{bmatrix}. \tag{2.1}$$

With $p = 0$ it corresponds to the central difference discretization; with $p = 1$ to the finite element discretization with piecewise linear test and trial functions. The discretization operator is used either with the given diffusion coefficient ε or with this coefficient replaced by an artificially enlarged diffusion coefficient $\alpha = \varepsilon + Ch$, where C is independent of ε and h.

Analogous to (2.1), for the one-dimensional problem we have

$$L_{h,\varepsilon} = \frac{+\varepsilon}{h^2}[1,-2,1] + \frac{2}{h}[-\tfrac{1}{2},0,\tfrac{1}{2}]$$

For the 1-D problem the discretization with artificial diffusion $\alpha = \varepsilon + h$ is equivalent with the usual upwind discretization.

3. MIXED DEFECT CORRECTION ITERATION

The iteration scheme we propose is a special case of the following "mixed defect correction iteration" - scheme (MDCP):

$$\text{(3.1a)} \qquad \tilde{L}_h^1 \, u_h^{(i+\frac{1}{2})} = \tilde{L}_h^1 \, u_h^{(i)} - L_h^1 \, u_h^{(i)} + f_h^1 ,$$

$$\text{(3.1b)} \qquad \tilde{L}_h^2 \, u_h^{(i+1)} = \tilde{L}_h^2 \, u_h^{(i+\frac{1}{2})} - L_h^2 \, u_h^{(i+\frac{1}{2})} + f_h .$$

In this process the operators L_h^1, L_h^2, $\tilde{L}_h^1$ and $\tilde{L}_h^2$ are discretizations of the operator L in the continuous problem

$$\text{(3.2)} \qquad Lu = f.$$

For the process (3.1) the following theorem is easily proved:

(3.3) THEOREM. *Let* $\tilde{L}_h^1$ *and* $\tilde{L}_h^2$ *satisfy the stability condition*:

$$\| \tilde{L}_h^{-1} \| < C, \text{ uniform in } h,$$

and let $L_h^k u_h = f_h$ *and* $\tilde{L}_h^k u_h = f_h$ *be discretizations of order* p_k *and* $q_k \leq p_k$ *respectively,* $k = 1,2$. *If for* (3.1) *a stationary solution*

$$u_h^A = \lim_{i \to \infty} u_h^{(i)}$$

exists, then

$$\| R_h u - u_h^A \| \leq C \, h^{\min(p_1+q_2, p_2)},$$

where $R_h u$ *is the restriction of the solution* u *of* (3.2) *to the grid.* □

For the convection diffusion equation (1.1) we make the following choice of operators in (3.1):

$$\text{(3.4)} \qquad \begin{aligned} L_h^1 &= L_{h,\varepsilon} \quad , \quad \tilde{L}_h^1 = L_{h,\alpha}, \\ L_h^2 &= L_{h,\alpha} \quad , \quad \tilde{L}_h^2 = D_{h,\alpha} = 2 \operatorname{diag}(L_{h,\alpha}). \end{aligned}$$

By these choices, (3.1a) is a defect correction step towards the 2nd order accurate solution of $L_{h,\varepsilon} u_h = f_h$, by means of the operator $L_{h,\alpha}$ as an approximation to $L_{h,\varepsilon}$. The second step (3.1b) is only a damped Jacobi-relaxation step towards the solution of the problem

$$L_{h,\alpha} u_h = f_h.$$

In the process (3.1)-(3.4) only linear systems for the discrete operator $L_{h,\alpha}$ have to be solved explicitly. For the treatment of these equations the multiple grid method

can be used. For details about this solution method we refer to VAN ASSELT (these proceedings). In this paper we shall only be concerned with the convergence of the iteration process (3.1)-(3.4) and with the properties of its fixed points (the "*stationary solutions*" of (3.1)).

After substitution of the operators (3.4) in the process (3.1), its two stationary solutions - if they exist -

$$u_h^A = \lim_{i\to\infty} u_h^{(i)} \quad \text{and} \quad u_h^B = \lim_{i\to\infty} u_h^{(i+\frac{1}{2})},$$

can be characterized as solutions of the linear equations

$$(3.5) \qquad [L_{h,\varepsilon} + (\alpha-\varepsilon)L_{h,\alpha} D_{h,\alpha}^{-1} \Delta_h] u_h^A = f_h,$$

$$(3.6) \qquad [L_{h,\varepsilon} + (\alpha-\varepsilon)\Delta_h D_{h,\alpha}^{-1} L_{h,\alpha}] u_h^B = [I + (\alpha-\varepsilon)\Delta_h D_{h,\alpha}^{-1}] f_h.$$

For a brief notation, we denote (3.5) also as

$$(3.7) \qquad M_{h,\varepsilon} u_h^A = f_h.$$

By means of theorem (3.2), it is easily shown that, for a fixed ε and $h \to 0$, the solution u_h^A is 1st order accurate, whereas u_h^B is 2nd order. With the aid of local mode analysis the behaviour of the solution can be analyzed more precisely.

4. LOCAL MODE ANALYSIS

To analyze the process (3.1)-(3.4) and its stationary solutions u_h^A and u_h^B, we use local mode analysis. For the one-dimensional model problem (1.2) the characteristic forms of the operators (3.4) are given by

$$(4.1) \qquad \hat{L}_{h,\varepsilon}(\omega) = \frac{-4\varepsilon}{h^2} S^2 + \frac{4i}{h} SC \quad \text{and} \quad D_{h,\alpha}(\omega) = \frac{-4\alpha}{h^2},$$

with $S = \sin(\omega h/2)$ and $C = \cos(\omega h/2)$. For $M_{h,\varepsilon}$ this results in the characteristic form

$$\hat{M}_{h,\varepsilon}(\omega) = \frac{-4\varepsilon}{h^2} S^2[1 + \frac{\alpha-\varepsilon}{\varepsilon} S^2] + \frac{4i}{h} SC[1 + \frac{\alpha-\varepsilon}{\alpha} S^2],$$

or, with the upwinding amount of artificial diffusion, $\alpha = \varepsilon + h$,

$$(4.2) \qquad \hat{M}_{h,\varepsilon}(\omega) = \frac{-4\varepsilon}{h^2} S^2[1 + \frac{h}{\varepsilon} S^2] + \frac{4i}{h} SC\,[1 + \frac{h}{h+\varepsilon} S^2].$$

For the two-dimensional problem (1.1) the characteristic forms are

(4.3) $$\hat{L}_{h,\varepsilon}(\omega) = \frac{-4\varepsilon}{h^2} S^2 + \frac{4i}{h} T, \qquad \hat{D}_{h,\alpha}(\omega) = \frac{-8\alpha}{h^2} \quad \text{and}$$

and

(4.4) $$\hat{M}_{h,\varepsilon}(\omega) = \frac{-4\varepsilon}{h^2} S^2[1 + \frac{\alpha-\varepsilon}{2\varepsilon} S^2] + \frac{4i}{h} T[1 + \frac{\alpha-\varepsilon}{2\alpha} S^2],$$

where

$$T = -[a_1 S_\phi (2C_\phi + pC_{\phi+2\theta}) + a_2 S_\theta (2C_\theta + pC_{\theta+2\phi})]/(4+2p),$$

$$S^2 = S_\phi^2 + S_\theta^2 , \; S_\phi = \sin\phi, \; C_\phi = \cos\phi ,$$

$$\phi = \omega_1 h/2 \text{ and } \theta = \omega_2 h/2.$$

Local consistency and stability of the operators is studied in HEMKER (1982). We recollect the following remarks (cf. also BRANDT, 1980). In the limit for $\varepsilon \to 0$, the continuous operator L_ε is unstable for the modes $u_\omega = e^{i\omega x}$ with frequencies $\omega = (\omega_1,\omega_2)$ that are perpendicular to $a = (a_1,a_2)$, i.e. for all modes with $\omega \perp a$ we have $a.\nabla u_\omega = 0$.

In the limit for $\varepsilon \to 0$, the discrete operator $L_{h,\varepsilon}$ is unstable for the modes $u_{h,\omega} = e^{i\omega h}$; for which ω satisfies $T(\omega) = 0$. In the finite difference discretization (p=0), these modes $\omega = (\omega_1,\omega_2)$ are simply characterized by

$$a_1 \sin(\omega_1 h) + a_2 \sin(\omega_2 h) = 0.$$

The operator $L_{h,\alpha}$ has no unstable modes for $\varepsilon \to 0$ and it is consistent (of order one) with $L_{\varepsilon,h}$ if and only if $|\alpha-\varepsilon| = O(h)$ as $h \to 0$.

Both in the 1-D and in the 2-D case (n = 1,2), the discretization (3.7) is consistent of order 2 and the operator $M_{h,\varepsilon}$ is *asymptotically stable*. Here we use the following

DEFINITION. The operator $M_{h,\varepsilon}$, a discretization of L_ε, is *asymptotically stable* if

(4.5) $$\forall \rho > 0 \;\; \exists \eta > 0 \;\; \forall \omega \in [-\pi/h,\pi/h]^n \;\; \lim_{\varepsilon\to 0} |\hat{L}_\varepsilon(\omega)| > \rho \Rightarrow \lim_{\varepsilon\to 0} \frac{|\hat{M}_{h,\varepsilon}(\omega)|}{|\hat{L}_\varepsilon(\omega)|} > \eta,$$

(cf. HEMKER, (1982). In the one dimensional case, n = 1, we even find that $M_{h,\varepsilon}$ is ε-uniformly stable, i.e. (4.5) is satisfied with η independent of ρ.

5. THE CONVERGENCE OF MDCP ITERATION

In this section we consider the rate of convergence for the MDCP iteration

(3.1)-(3.4). By local mode analysis we show at what rate the different frequencies in the error are damped in the process, when the stationary solutions u_h^A and u_h^B are computed. The transition matrices of the defect correction step (3.1,a) and the damped Jacobi step (3.1,b) have the following characteristic forms

$$\hat{R}^{DCP}(\omega) = \widehat{(\tilde{L}_h^1 - L_h^1)}(\omega)/\hat{\tilde{L}}_h^1(\omega) = (\alpha-\varepsilon)\hat{\Delta}_h(\omega)/\hat{L}_{h,\alpha}(\omega),$$

$$\hat{R}^{JAC}(\omega) = \widehat{(\tilde{L}_h^2 - L_h^2)}(\omega)/\hat{\tilde{L}}_h^2(\omega) = (\hat{L}_{h\alpha}(\omega) - \hat{D}_{h,\alpha})/\hat{D}_{h,\alpha}.$$

The MDCP transition operator reads

$$\hat{R}^{MDCP}(\omega) = \hat{R}^{DCP}(\omega).\hat{R}^{JAC}(\omega).$$

For the one-dimensional model problem we find

$$(5.1) \qquad \hat{R}^{MDCP}(\omega) = \frac{(\alpha-\varepsilon)SC}{-\alpha} \quad \frac{[SC(\alpha^2-h^2)+ih\alpha]}{\alpha^2S^2+h^2C^2},$$

and

$$(5.2) \qquad |\hat{R}^{MDCP}(\omega)| \le \frac{\alpha-\varepsilon}{\alpha} \tfrac{1}{2}\sqrt{\tfrac{1}{4}(\tfrac{\alpha}{h} - \tfrac{h}{\alpha})^2 + \max^2(\tfrac{h}{\alpha}, \tfrac{\alpha}{h})}.$$

With the upwinding amount of artificial viscosity, $\alpha = \varepsilon + h$, we find

$$|\hat{R}^{MDCP}(\omega)| \le \frac{1}{2}\frac{1}{\varepsilon+h}\sqrt{(\varepsilon+h)^2+\varepsilon^2} \le \tfrac{1}{2}\sqrt{2} < 1.$$

i.e. the process converges with a finite rate for all frequencies. In the limit for $\varepsilon \to 0$ we find

$$|\hat{R}^{MDCP}(\omega)| \le \frac{1}{2}.$$

The slowest convergence rate is shown for the intermediate frequencies ($\omega = \pm \pi/2h$); both the low and the high frequencies damp much faster.

For the 2-D problem the situation is somewhat more complex; we find

$$(5.3) \qquad |\hat{R}^{MDCP}(\omega)| = \frac{(\alpha-\varepsilon)S^2\sqrt{(\frac{\alpha}{h}C^2S^2 - \frac{h}{\alpha}T^2)^2 + 4T^2)}}{2h \qquad [(\frac{\alpha}{h}S^2)^2 + T^2]},$$

where $C^2 = C_\phi^2 + C_\theta^2$. It is easy to show that $|\hat{R}^{MDCP}(\omega)| \le 1$ for all ω. However, for some frequencies convergence is slow. E.G. for the unstable modes ω of $L_{h,\varepsilon}$, for which $T(\omega) = 0$, we find

$$|\hat{R}^{MDCP}(\omega)| = \frac{\alpha-\varepsilon}{2\alpha}(C_\phi^2 + C_\theta^2),$$

i.e. for small ε, along $T(\omega) = 0$, in the neighbourhood of $\omega = 0$, convergence is slow. If we set $\alpha = \varepsilon + \gamma h$, then, considering the limit for $\varepsilon \to 0$, we obtain

$$(5.4) \qquad |\hat{R}^{MDCP}(\omega)| = \left|\frac{\gamma S^2}{T}\right| \frac{\sqrt{1 + \frac{1}{4}\left(\frac{T}{\gamma} - C^2\left(\frac{\gamma S^2}{T}\right)\right)^2}}{1 + \left(\frac{\gamma S^2}{T}\right)^2}$$

To understand this expression, we introduce a new coordinate system in the frequency space. We define lines with constant $y = \gamma S^2(\omega)/T(\omega)$ and lines with constant $t = T(\omega)/\gamma$. Then

$$(5.5) \qquad |\hat{R}^{MDCP}(\omega)| = \frac{y}{1+y^2} \sqrt{1 + \frac{1}{4}(t-(2-yt)y)^2} .$$

In the neighbourhood of the origin lines of constant y are approximately circles, tangent in the origin to the line $T(\omega) = 0$, the value of y is proportional to the radius. Lines of constant t are lines approximately parallel to the line $a_1\omega_1 + a_2\omega_2 = 0$, t is proportional to the distance to this line.

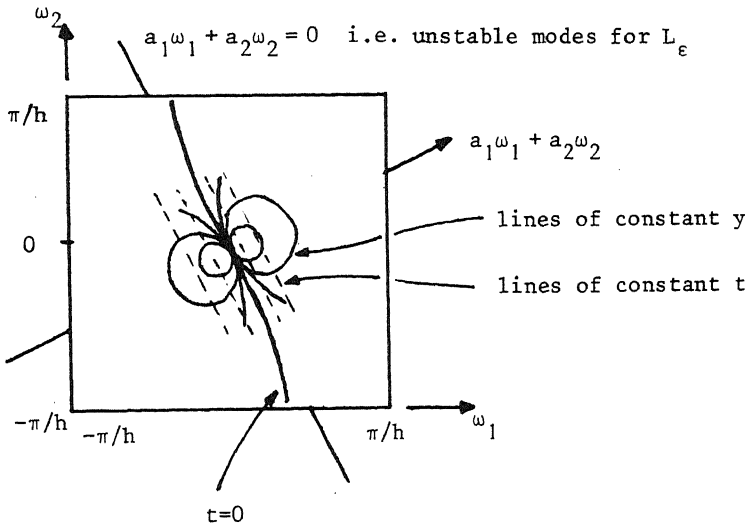

Figure 1. Lines of constant $y = \gamma S^2/T$ and constant $t = T/\gamma$ in the frequency space.

From (5.5) we see

(i) for small y

$$|\hat{R}^{MDCP}(\omega)| \approx y\sqrt{1 + \frac{1}{4}t^2} = O(y);$$

(ii) for large y, i.e. in the neighbourhood of t = 0,

$$|\hat{R}^{MDCP}| \approx \sqrt{y^{-2} + \frac{1}{4}C^2} \approx \frac{1}{2}(C_\phi^2 + C_\theta^2).$$

We see that low frequencies converge fast along the convection direction $\vec{a}$ and that convergence is slow (only!) in the direction perpendicular to the convection direction (i.e. for those ω with $T(\omega) = 0$). In figure 2 we give an impression of the MDCP convergence rate as a function of ω. In this figure the rate is shown for the finite difference discretization (e.g. (2.1) with p = 0). The same behaviour is seen for the finite element discretization (p = 1). For other convection directions $\vec{a}$ the sharp ridge at the origin turns around the origin correspondingly.

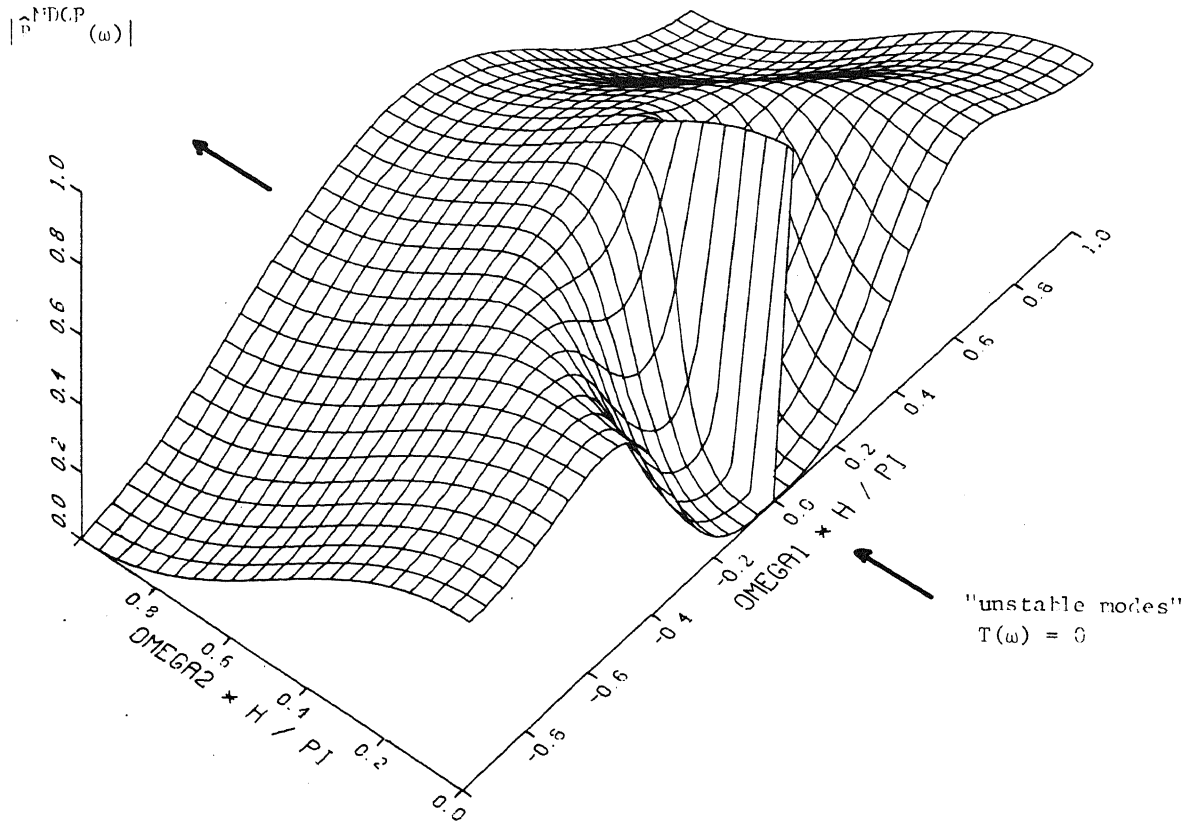

Figure 2. The MDCP convergence rate for the equation $-\varepsilon\Delta u + u_x = f$.

6. BOUNDARY ANALYSIS OF THE MDCP SOLUTION

Away from the boundary we already know that the MDCP discretization is asymptotically stable with respect to the right-hand side f_h. To analyze the effects of the boundary data, we consider the homogeneous problem

$$Lu_\omega = 0$$

in a discretization of the right half-space ($x \geq 0$), the boundary $x = 0$ being a grid-line. Dirichlet boundary data are given on this boundary and we consider solutions that are bounded at infinity. This situation is again studied by mode analysis, cf. BRANDT (1980). Now we use complex modes, $\omega = (\omega_1, \omega_2) \in \mathbb{C}^2$; $\omega_2 \in \mathbb{R}$ is given by the boundary data and $\hat{L}_h(\omega) = 0$ is solved for $\omega_1 \in \mathbb{C}$. Those solutions ω_1 for which $\operatorname{Im} \omega_1 > 0$ determine the behaviour of the discretization near the boundary at $x = 0$.

In this way, we first treat the one-dimensional model problem (1.2) with $\alpha = \varepsilon + h$. For this problem the only possible inhomogeneous boundary data are $u_h(0) = 1$. The modes

$$u_{h,\omega}(jh) = e^{i\omega hj} = \lambda^j$$

for which $M_{h,\varepsilon}\, u_{h,\omega} = 0$ are determined by

$$\hat{M}_{h,\varepsilon}(\omega) = 0, \tag{6.1}$$

which is a 4th degree polynomial in λ. In the limit for $\varepsilon \to 0$ we find for (6.1) the solutions $\lambda = 1$, $\lambda = 0$, $\lambda = 2 \pm \sqrt{5}$. From (4.2) it is clear that for all $\varepsilon/h > 0$, $\lambda = 1$ is a solution and no other solutions with $|\lambda| = 1$ exist. Since all λ are continuous functions of ε, we have for all $\varepsilon \geq 0$ two λ's with $|\lambda| < 1$ and two λ's with $|\lambda| \geq 1$. The two λ's with $|\lambda| < 1$ determine the behaviour of the solution near the boundary at $x = 0$. For small values of ε/h we find

$$\lambda_1 = \frac{3}{2}\frac{\varepsilon}{h} + O((\frac{\varepsilon}{h})^2)$$

and

$$\lambda_2 = 2 - \sqrt{5} - (2 - \frac{2}{5}\sqrt{5})(\frac{\varepsilon}{h}) + O((\frac{\varepsilon}{h})^2)$$

$$\approx -0.236.$$

These values show that in the numerical boundary layer, for small ε/h, the influence of the boundary data decreases with a fixed rate per meshpoint. I.e. the width of

the numerical boundary layer is only $O(h)$.

Of course, λ_1 and λ_2 only determine what modes appear in the solution of

$$M_{h,\varepsilon}\, u_h = 0 \qquad u_h(0) = 1;$$

their relative amount is determined by the difference operator in the mesh-point next to the boundary. A closed analysis shows

$$\begin{aligned} u_h^A(jh) &= -(2+2\sqrt{5})\,\frac{\varepsilon}{h}\,\lambda_1^j + [1 + (2+2\sqrt{5})\frac{\varepsilon}{h}]\lambda_2^j + O((\tfrac{\varepsilon}{h})^2), \\ u_h^B(jh) &= -(\tfrac{1}{2}+\tfrac{1}{2}\sqrt{5})\,\lambda_1^j + (\tfrac{3}{2}+\tfrac{1}{2}\sqrt{5})\lambda_2^j + O((\tfrac{\varepsilon}{h})). \end{aligned} \tag{6.2}$$

This describes completely the behaviour of the 1-D numerical boundary layer solution.

For the 2-D model problem we proceed similarly. For given boundary data

$$u_{h,\omega}(jh) = e^{i\bar{\omega}h_2 j_2} \qquad \text{for } j_1 = 0,$$

we compute the modes

$$u_{h,\omega}(jh) = e^{i\omega h j} = e^{i\omega_1 h_1 j_1}\, e^{i\omega_2 h_2 j_2} = \lambda^{j_1}\, e^{i\bar{\omega}h_2 j_2},$$

that satisfy

$$M_{h,\varepsilon}\, u_{h,\omega} = 0 \qquad \text{for } j_1 > 0,$$

and we determine the corresponding $|\lambda|$.

To simplify the computation, we restrict ourselves to the finite difference star ($p = 0$) and artificial diffusion $\alpha = \varepsilon + h\,|a_1|/2$, $a_1 \neq 0$. First we consider boundary data with $\bar{\omega} = 0$ fixed. In the limit for $\varepsilon/h \to 0$ we determine λ from

$$\hat{M}_{h,0}(\omega) = 0\ .$$

We find the solutions $\lambda_0 = 0$, $\lambda_1 = 1$, $\lambda_{2,3} = 3 \pm \sqrt{12}$. Next we consider $\bar{\omega} \neq 0$. From (4.4) with $\varepsilon = 0$,

$$\hat{M}_{h,0}(\omega) = \frac{-2\alpha}{h^2}\, S^4 + \frac{2i}{h}\, T[2+S^2], \tag{6.3}$$

it follows that no real $\omega \in [-\pi/h, \pi/h]^2$, $\omega \neq (0,0)$, exists such that $\hat{M}_{h,0}(\omega) = 0$. Hence, except for $\bar{\omega} = 0$, no λ exists with $|\lambda| = 1$. All λ's are continuous functions of $\bar{\omega}$ and for small $\bar{\omega}$ we know

$$\lambda_1 = 1 - i\,\frac{a_2}{a_1}\,\bar{\omega}h + O((\bar{\omega}h)^4).$$

Hence $|\lambda_1| \geq 1$ and for all $\bar{\omega} \in [-\pi/h, \pi/h]$ there are two λ's with $|\lambda| < 1$ and two λ's with $|\lambda| \geq 1$. The two small λ's, considered as functions of $\bar{\omega} \in [-\pi/h, \pi/h]$ describe a curve inside the unit circle in C. These curves are closed subsets of $\mathbb{C}$ and have no point in common with the unit-circle. Thus, we see that $C = \max_{\bar{\omega}} |\lambda_{\bar{\omega}}|$ exists and

$$|\lambda| \leq C < 1.$$

If, instead of (6.3), we take (4.4) with $\varepsilon \neq 0$ as a starting point, the same continuity argument yields the same result for all ε which satisfy $0 \leq \varepsilon \leq Ch$. We conclude that, also in the two-dimensional case for small ε/h, the influence of the boundary data decreases with a fixed rate per meshpoint, i.e. the width of the numerical boundary layer is $O(h)$.

The above, non-constructive proof for the existence of $\max_{\bar{\omega}} |\lambda_{\bar{\omega}}| < 1$, allows the possibility of a large $|\lambda_{\omega}| < 1$, such that the existence $\bar{\omega}$may be of little practical use. In the numerical examples we show that the numerical boundary layer extends only over a few meshlines in the neighbourhood of the boundary indeed.

7. NUMERICAL RESULTS

In this section we show two numerical examples. The first example is to demonstrate the $O(h)$-width of the numerical boundary layer in the downstream direction. In the 2nd example we show that MDCP-iteration can also be applied to problems with interior layers and with variable coefficients. In both problems we discretize by the finite element method with piecewise linear test- and trial functions on a regular triangularization. The solution of the linear systems is obtained by a multiple grid method that is fully consistent with the finite element discretization. It used the 7-point Incomplete LU-relaxation, the 7-point prolongation and the 7-point restriction of which the weights are properly adapted to the Dirichlet or Neumann boundary conditions; no additional artificial diffusion is applied on coarser levels.

EXAMPLE 1.

We solve the constant coefficient problem

$$\varepsilon\Delta u + u_x = f(x,y),$$

on the unit square with Dirichlet boundary conditions. The boundary data and the data $f(x,y)$ are chosen such that

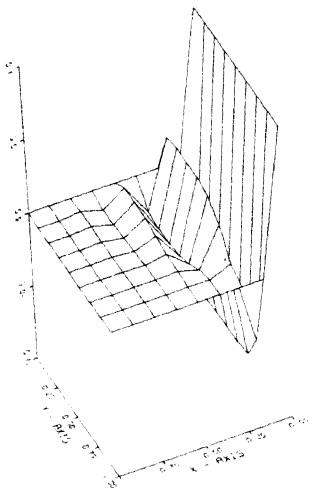

Fig. 3a

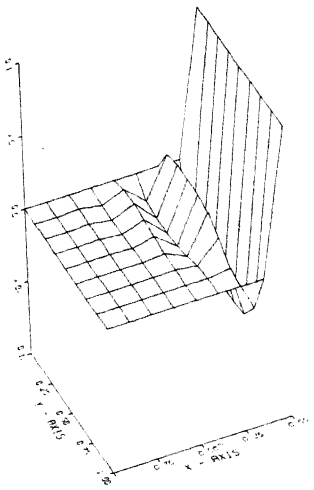

Fig. 3a'

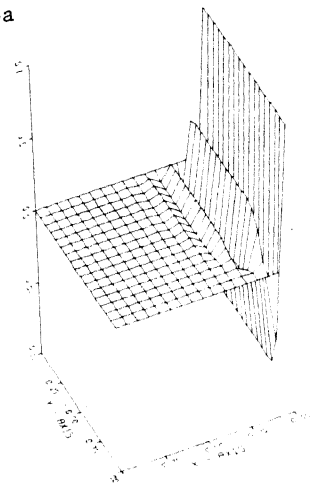

Fig. 3b

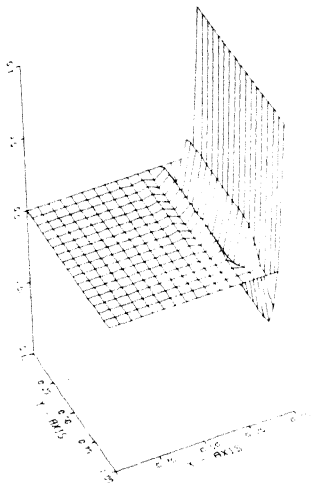

Fig. 3b'

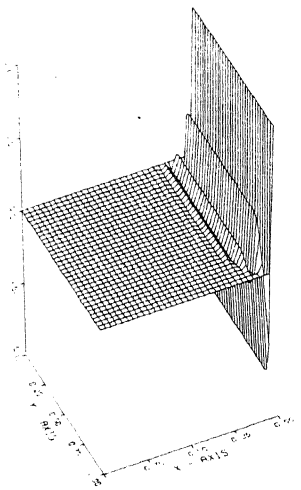

Fig. 3c

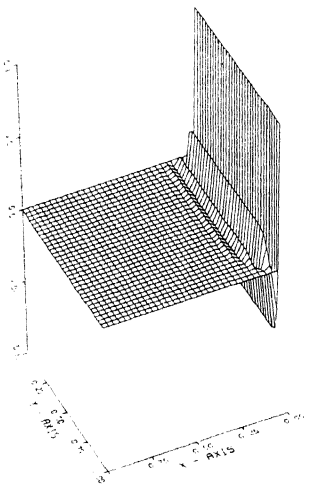

Fig. 3c'

Fig. 3 The numerical boundary layer in example 1.

$$u(x,y) = (\exp(-x/\varepsilon) - \exp(-1/\varepsilon))/(1-\exp(-1/\varepsilon)).$$

This solution only shows the exponential boundary-layer near the down-stream boundary. No smooth components in the solution are present. (In HEMKER (1982) we showed that smooth components - if present - are represented with an accuracy of order $O(h^2)$).

In the figures 3a, 3b, 3c, 3a', 3b', 3c' the solutions u_h^A and u_h^B as obtained by the MDCP-iteration are shown for mesh-widths h = 1/8, h = 1/16, h = 1/32. We see that the numerical boundary layer extends over a fixed number of mesh-lines away from the down-stream boundary, regardless of the meshwidth used.

EXAMPLE 2.

This second example describes a circular flow around a point. The equation reads

$$-\varepsilon\Delta u + \vec{b}.\nabla u = 0 \qquad \text{on } [-1,+1] \times [0,1]$$

$$\vec{b} = (2y(1-x^2),\ -2x(1-y^2))^T.$$

The boundary data are

(i) a Dirichlet boundary condition on $-1 \le x \le 0$, $y = 0$

$$u(x) = D(x) = 1 + \tanh(\gamma(1+2x)),$$

$$\gamma = 10,$$

and (ii) homogeneous Neumann boundary conditions on the remaining part of the boundary.

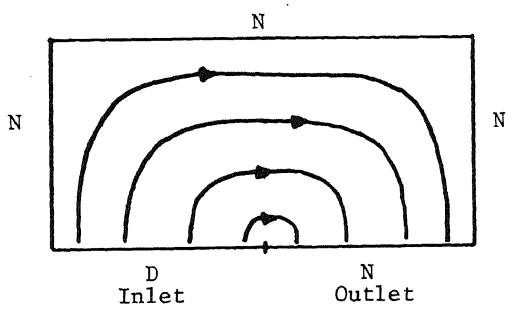

The convection direction is clockwise around the origin; the Dirichlet boundary condition is given at the upstream boundary, whereas the other boundary conditions are of Neumann type. The Dirichlet boundary data are such that s sharp interior layer is created in the interior of the domain. In the limit for $\varepsilon \to 0$, the exact solution at the outflow boundary is

$$u(x,0) = D(-x) \qquad 0 \le x \le 1.$$

The discretization is made on a regular grid with $h = 1/16$ and with $\varepsilon = 10^{-6}$.

In Figure 4 we compare the shapes of the outflow profile for 4 numerical solutions. One solution is obtained by straightforward application of artificial diffusion, $\alpha = \varepsilon + h/2$. (For a smaller artificial diffusion $\alpha = \varepsilon + h/4$ the MG-method for the solution of the system

$$L_{h,\alpha}\, u_h = f_h$$

diverges.) The other 3 solutions are obtained by MDCP-iteration. (At the outflow boundary both solutions u_h^A and u_h^D coincide!). These solutions are computed for different values of the artificial diffusion viz. $\alpha = \varepsilon + 2h$, $\alpha = \varepsilon + h$ and $\alpha = \varepsilon + h/2$.

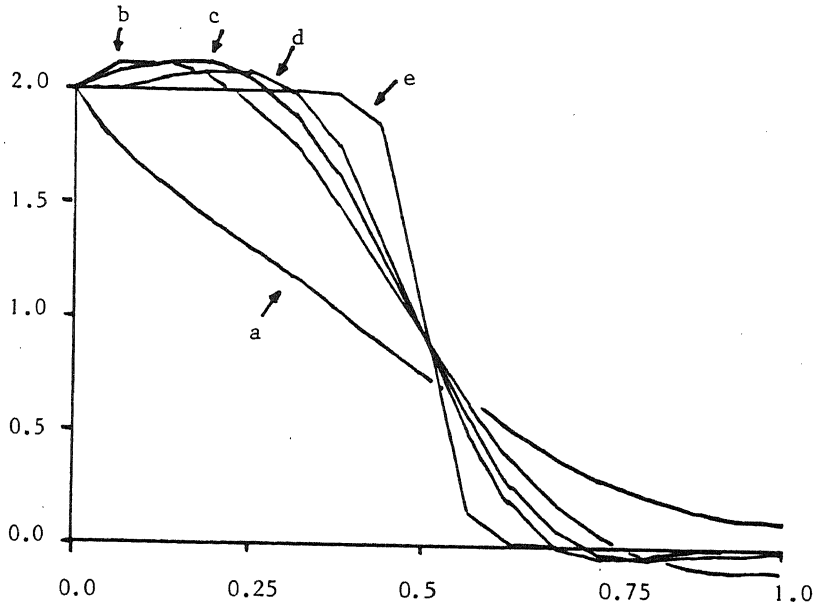

Figure 4. The outflow profile $u_h(x,0)$ in example 2.
a) artificial diffusion solution $\alpha = \varepsilon + h/2$
b) MDCP-iteration $\alpha = \varepsilon + 2h$,
c) $\alpha = \varepsilon + h$,
d) $\alpha = \varepsilon + h/2$,
e) pointwise exact limit-solution for $\varepsilon \to 0$.

In figure 4 we see that the interior layer is very well transported through the interior domain. Smaller values of the artificial diffusion in MDCP-iteration yield more accurate solutions.

EXAMPLE 3.

This example uses the same equation as example 2. Here the boundary conditions are

(i) Dirichlet boundary conditions

$$\begin{aligned} u(x) &= D(x) \quad \text{on } -1 \le x \le 0 \quad , \quad y = 0, \\ u(x) &= 0 \quad \text{on } -1 \le x \le +1 \qquad y = 1, \\ u(x) &= 0 \quad \text{on } 0 \le y \le 1 \qquad x = \pm 1; \end{aligned}$$

and

(ii) homogeneous Neumann boundary conditions at the outlet boundary

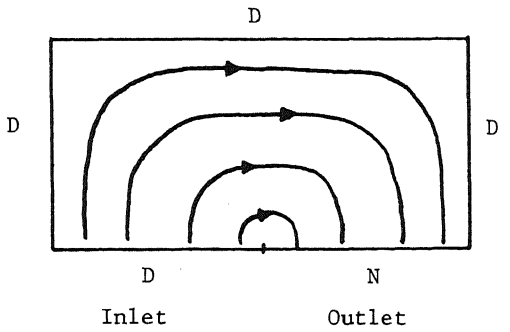

In figure 5a and 5b we give an impression of the numerical solution u_h^A and u_h^B obtained by MDCP-iteration and in figure 5c of the numerical solution obtained by artificial diffusion only. In figure 5d we show the computed solution that is obtained by application of one single defect correction step (3.1a) to correct the artificial diffusion solution as shown in fig. 5c. For all figures $\alpha = \varepsilon + h/2$ was used. From the figures we see that MDCP-iteration yields a better solution than is found by simple defect correction only, although both are theoretically 2nd order approximations.

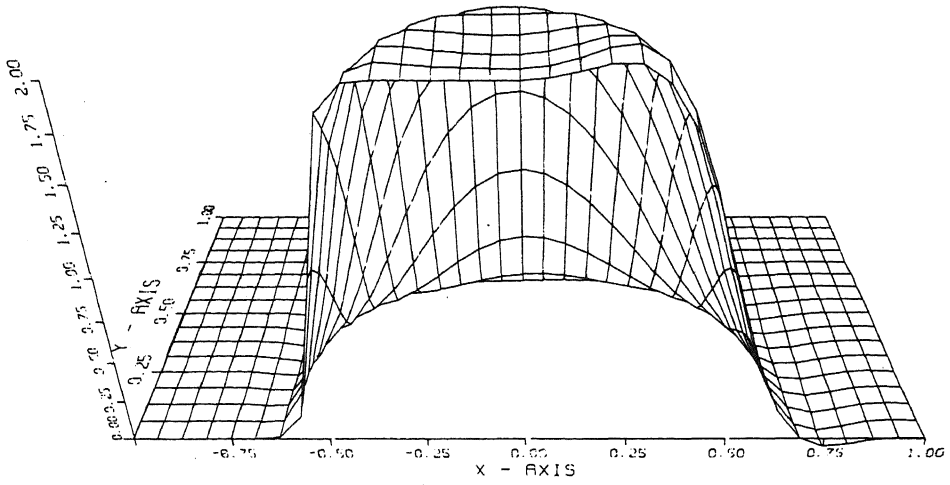

Fig. 5a The solution u_h^A in example 3

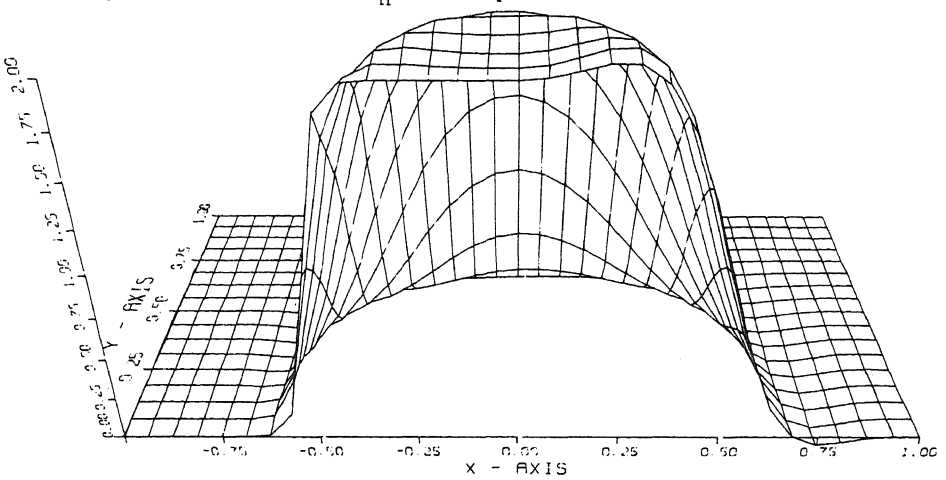

Fig. 5b The solution u_h^B in example 3

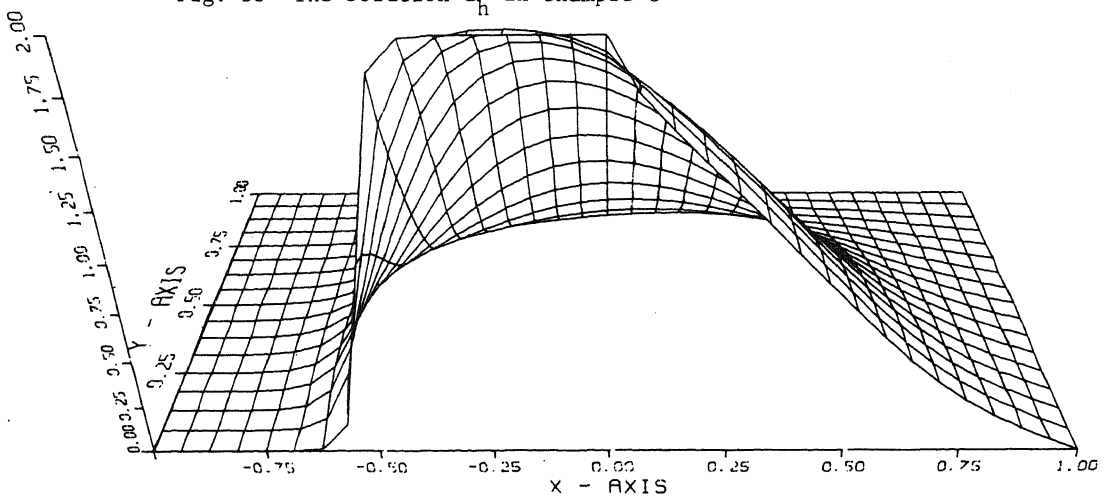

Fig. 5c The artificial diffusion solution in example 3

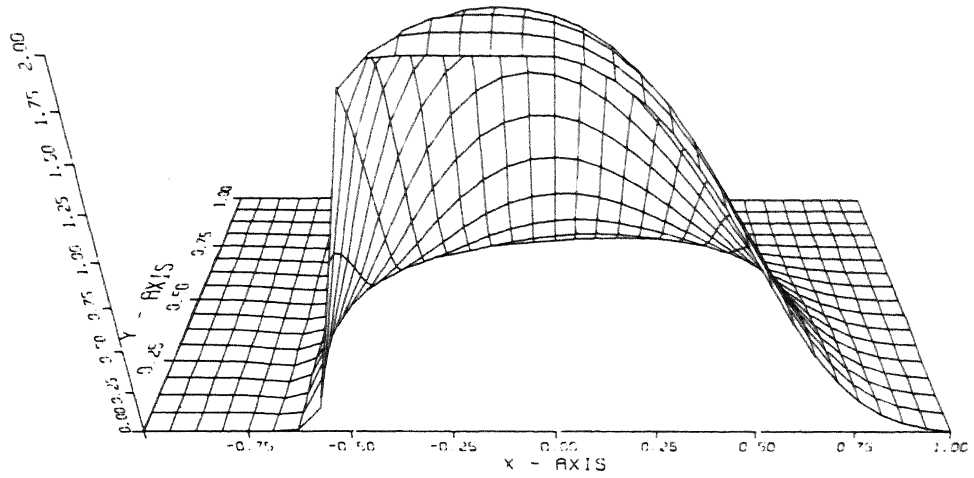

Fig. 5d The numerical solution of example 3 obtained by a single defect correction iteration step applied to the solution in figure 5c.

REFERENCES

BRANDT, A. [1980] *Numerical stability and fast solutions to boundary value problems.* in: Boundary and Interior Layers - Computational and asymptotic methods (J.J.H. Miller ed.) Boole Press, Dublin, 1980.

HACKBUSCH, W. [1979], *Bemerkungen zur iterierten Defektkorrektur und zu ihrer Kombination mit Mehrgitten verfahren.* Report 79-13, Math. Inst. Univ. Köln, 1979.

HEMKER, P.W. [1981], *Introduction to multi-grid methods,* Nw. Arch. Wisk. 29 (1981) 71-101.

HEMKER, P.W. [1982], *An accurate method without directional bias for the numerical solution of a 2-D elliptic singular perturbation-problem.* Procs. Oberwolfach meeting on Singular Perturbation Problems, to appear in Springer LNM, 1982.

STETTER, H. [1978], *The defect correction principle and discretization methods.* Num. Math. 29 (1978) 425-443.